THE JOURNAL OF COMPARATIVE NEUROLOGY 474:261–275 (2004)

Paucity of Horizontal Connections for Binocular Vision in V1 of Naturally Strabismic Macaques: Cytochrome Oxidase Compartment Specificity

LAWRENCE TYCHSEN,[1,2]* AGNES MING-FONG WONG,[1] AND ANDREAS BURKHALTER[2]

[1]Departments of Ophthalmology and Visual Sciences, Washington University School of Medicine, St. Louis, Missouri 63110

[2]Departments of Anatomy and Neurobiology, Washington University School of Medicine, St. Louis, Missouri 63110

ABSTRACT

To describe the structural basis for lack of binocular fusion in strabismic primates, we investigated intrinsic horizontal connections within striate cortex (area V1) of normal and strabismic, adult macaque monkeys. The strabismic animals had early-onset natural esotropia (the visual axes deviated nasally), normal visual acuity in each eye, and the constellation of ocular motor deficits that typify human infantile strabismus. Horizontal patchy connections and synaptic boutons were labeled by injections of the neuronal tracer biotinylated dextran amine. Ocular dominance columns (ODCs), and blob vs. interblob compartments, were revealed by using cytochrome oxidase (CO). In layers 2/3 and 4B of the strabismic monkeys, patchy projections and boutons terminated much more frequently in same-eye (73%) as opposed to opposite-eye (27%) ODCs (normal monkeys 58% and 42%, respectively). The deficiency of binocular connections in the strabismic cortex was evident qualitatively as a "skip" pattern, in which every other row of ODCs had labeled patches. Analysis of V1 in normal monkeys revealed that the deficits in strabismic V1 were due mainly to a loss of binocular connections between neurons in CO-interblob compartments. In both normal and strabismic monkeys: (1) CO-blob compartment neurons showed a more pronounced bias for monocular connectivity, and (2) commitment of connections to the same CO-compartment as the injection site (blob-to-blob, or interblob-to-interblob) was moderately strong (64%) but far from absolute. These findings help elucidate the relative roles of visual experience vs. innate mechanisms in the development of axonal connections between ocular dominance domains and compartments within macaque V1. They also provide the first detailed description of the V1 maldevelopments associated with unrepaired natural, infantile-onset strabismus in primates. J. Comp. Neurol. 474:261–275, 2004.

Indexing terms: Area V1; cytochrome oxidase blobs; laminar connections; binocular fusion; congenital esotropia

Binocular vision is made possible by connections within area V1 that allow sharing of information between the two eyes. The connections are necessary because the geniculocortical input into V1 is completely segregated into right

Grant sponsor: Research to Prevent Blindness, Inc. (L.T.)/Walt and Lilly Disney Award; Grant sponsor: National Institutes of Health; Grant number: P01 NS 17763-12 (A.B., L.T); Grant sponsor: Human Frontiers Science Program Organization (A.B.); Grant number: #RG-93; Grant sponsor: National Eye Institute of the National Institute of Health (LT); Grant number: EY10214-01A2; Grant sponsor: Research to Prevent Blindness; Grant number: unrestricted grant to the Department of Ophthalmology and Visual Sciences.

*Correspondence to: Lawrence Tychsen, St. Louis Children's Hospital, One Children's Place, Room 2 South 89, St. Louis, MO 63110.
E-mail: tychsen@vision.wustl.edu

Received 22 May 2003; Revised 3 December 2003; Accepted 30 January 2004

DOI 10.1002/cne.20113

Published online in Wiley InterScience (www.interscience.wiley.com).

TABLE 1. Ocular History and Characteristics of Macaque Monkeys Used in These Experiments

Animal	Age / sex / weight	Species	History	Ocular alignment	Refractive error
AR	10 yr / M /12 kg	*M. nemestrina*	Natural strabismus onset < 4 wks	Alternating esotropia 25 deg	RE + 3.00 + 0.50 × 180 LE + 1.75
LA	14 yr / F/ 12 kg	*M. mulatta*	Natural strabismus onset < 4 wks	Alternating esotropia 18 deg	RE + 2.50 + 1.00 × 010 LE + 5.00 + 2.00 × 170
ER	6 yr / M / 11 kg	*M. arctoides*	Normal	Orthotropic	RE + 2.50 LE + 2.00
ME	8 yr / M /8 kg	*M. nemestrina*	Normal	Orthotropic	RE + 1.00 LE − 0.50 + 1.50 × 020

RE, right eye; LE, left eye.

eye and left eye columns (Hubel and Wiesel, 1968, 1969). The presence of binocular connections was first inferred from physiological recordings, which showed that the bulk of neurons within an ocular dominance column (ODC) above and below layer 4 could be driven by input to either eye (Hubel and Wiesel, 1968). Despite the functional importance of binocular vision, little neuroanatomic information has emerged in the ensuing quarter century about horizontal connections for binocularity in primates.

It is well established that area V1 contains horizontal axonal connections that are long enough to join ODCs and that are organized in functionally important ways. The first descriptions of local connections were made by examining silver-stained sections of degenerating axons in V1 after electrolytic lesions (Fisken et al., 1973, 1975). A decade later Rockland and Lund (1983) injected horseradish peroxidase (HRP) into V1 and reported lattice-like networks of horizontal axons, which in flattened sections could be seen to consist of patches or clusters of axons radiating outward from neuronal somata at the injection center. The distribution of the patchy connections was subsequently shown to be semispecific, tending to join neurons in CO-rich blobs (or CO-patches; Horton and Hubel, 1981) to neurons in other blobs, and interblobs to interblobs, for processing of color and form information (Livingstone and Hubel, 1984b; Ts'o et al., 1986; Lund et al., 1993).

Single unit recordings from layer 2/3 of V1 and labeling of patchy connections indicate that blob neurons differ from interblob neurons in binocular connectivity. Only ~60% of blob neurons but ~80% of interblob neurons can be driven by input to either eye (i.e., neurons falling into ocular dominance groups 2–6; Livingstone and Hubel, 1984b). Similar biases are apparent in biocytin-labeled patchy connections, with the majority of blob neurons connecting to blob neurons of the same ocularity (Malach et al., 1993; Yoshioka et al., 1996). Recordings in V1 have also revealed differences in binocularity between layers 2/3 and 4B, with fewer binocularly responsive but more directionally selective neurons in layer 4B (Livingstone and Hubel, 1984b; Van Essen, 1985; Hawken et al., 1988).

Detailed knowledge of binocular connections in V1 is important not only for a more complete understanding of normal vision in primates, but also for understanding the neural mechanisms underlying visual disorders. Strabismus is an important pediatric visual disorder, depriving ~5% of children of the benefits bestowed by normal binocular vision (Rubenstein et al., 1985). Of all subtypes of pediatric strabismus, infantile esotropia (convergent strabismus) is the most important but least understood. It is important to clinicians because it is difficult to treat, often requiring multiple surgical procedures to restore stable eye alignment (von Noorden, 1996). It is important to vision scientists because it is known to be associated with profound deficits in visual processing for vergence eye movements (Tychsen and Scott, 2003), stereopsis (Birch and Stager, 1985; Birch et al., 1990), motion perception (Tychsen and Lisberger, 1986; Norcia et al., 1991; Tychsen et al., 1996; Schor et al., 1997), and smooth pursuit eye movement (Schor and Levi, 1980; Tychsen et al., 1985; Tychsen and Lisberger, 1986; Kiorpes et al., 1996; Schor et al., 1997).

A century ago, clinicians postulated a deficiency of binocular connections in infants who develop esotropia shortly after birth (Worth, 1903; Chavasse, 1939). Deficits in binocular connections have been reported in kittens reared with unilateral strabismus created by the sectioning of one eye muscle (Lowel and Singer, 1992; Trachtenberg and Stryker, 2001). To examine connections in primates with natural strabismus (Kiorpes and Boothe, 1981), we labeled long-range horizontal projections in area V1 of macaque monkeys who developed esotropia shortly after birth. The compartmental distribution of patchy connections and the number of synaptic boutons in layers 2/3 and 4B of the strabismic monkeys were compared with those measured in control macaques who had normal eye alignment.

MATERIALS AND METHODS

Animals

Experiments were performed on two naturally strabismic and two normal adult macaque monkeys (Table 1). The strabismic monkeys developed esotropic strabismus spontaneously before age 4 weeks (Kiorpes and Boothe, 1981), as documented by R.G. Boothe at the Yerkes Regional Primate Center in Atlanta, Georgia. Cycloplegic refractions performed in infancy revealed moderate hyperopia, suggesting that the animals had infantile esotropia with a refractive (accommodative) component. At adult age, the monkeys were shipped to Washington University in St. Louis where they were trained to fixate small tracking targets by using positive-feedback rewards. Eye movement recordings showed the constellation of ocular motor signs that typify human infantile strabismus (Tychsen et al., 2000): constant, nonparalytic esotropia of 18–25 degrees; fixation that spontaneously alternated between the right and left eye (i.e., no significant amblyopia); low-velocity latent nystagmus when fixating stationary targets; and a directional asymmetry of horizontal smooth pursuit under conditions of monocular viewing favoring target motion that was nasally directed in the visual field. Funduscopic examination was normal, with no evidence of

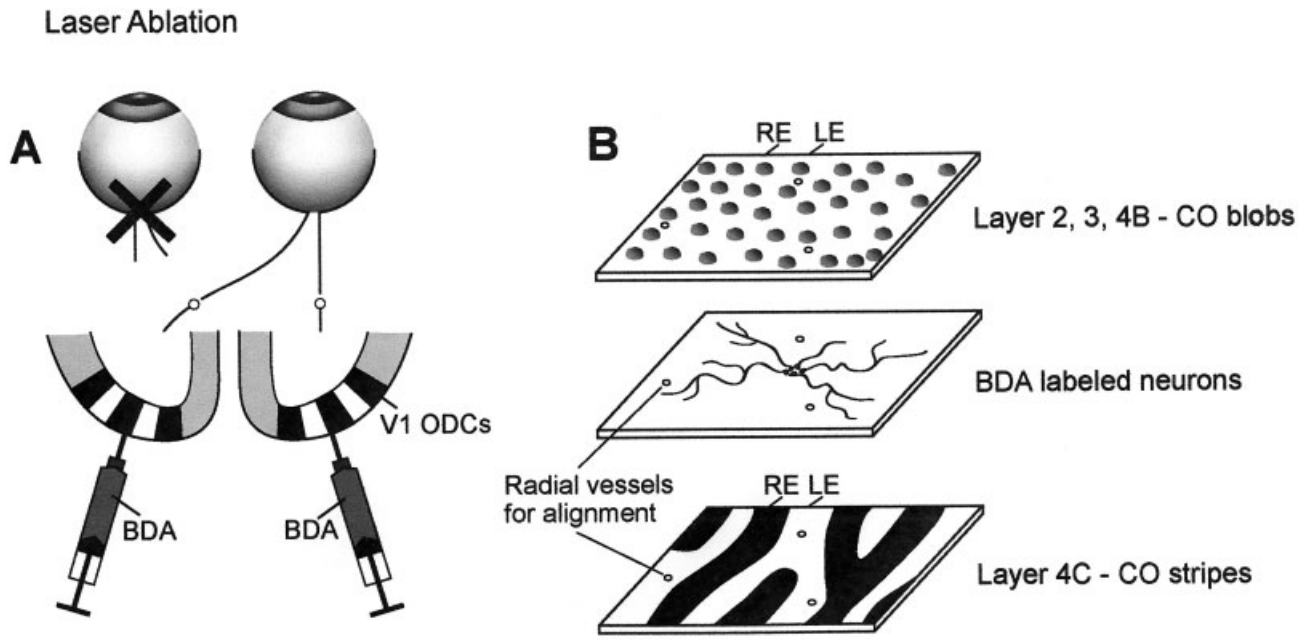

Fig. 1. **A:** Double-labeling method used in the experiments. A laser was used to deafferentate one eye, causing down-regulation of cytochrome oxidase (CO) activity in ocular dominance column (ODC) layer 4C neurons driven by the deafferented eye. Biotinylated dextran amine (BDA) was then injected into V1 in an attempt to hit right and left eye ODCs. Over a survival time of 3 days, BDA was taken up by neuronal somata at the injection site and anterogradely transported to their axonal terminations. **B:** The relationship between BDA-labeled axonal projections and V1 ODCs was analyzed by superimposing adjacent tangential sections stained to reveal CO blobs of layer 2/3, BDA in layers 2–4, and CO stripes of layer 4C. Radial blood vessels were used to align vertically adjacent sections.

ocular albinism. Two monkeys who had normal eye alignment and eye movements served as controls. One strabismic monkey (AR) of the current study had preliminary counts of boutons reported in a clinical journal (Tychsen and Burkhalter, 1995). Strabismic monkey AR and normal monkey ME had measurement of ODC widths reported in an earlier study (Tychsen and Burkhalter, 1997). The experimental protocol was approved by the Washington University Animal Care and Use Committee and conformed to NIH guidelines.

Overview of anatomic methods

A double-labeling technique was used to reveal binocular connections. To produce ODC stripes in layer 4C of V1, one eye in each animal was deafferented using a laser (Hoyt and Luis, 1962) to cause down-regulation of cytochrome oxidase (CO) activity in neurons dominated by input of that eye (Fig. 1A). Biotinylated dextran amine (BDA) was then injected into V1 to label intracortical axonal projections. After a short survival time (7 days) to permit the down-regulation of CO activity in layer 4C and transport of BDA in layers 2–4 (Fig. 1B), the animals were perfused with fixative and the occipital lobes removed for histological processing. Previous experiments in normal and strabismic macaques documented that laser deafferentation does not cause down-regulation/shrinkage of CO-blobs in layers 2–4B during this short survival time (Tychsen and Burkhalter, 1997).

Laser deafferentation

The monkeys were sedated with ketamine hydrochloride (10 mg/kg i.m.) and atropine (0.04 mg/kg i.m.). The pupils were dilated with mydriatic eye drops. The left eye was deafferented by applying ~150–200 spot burns (200 mW, 200 msec per burn) to the optic disc using an indirect ophthalmoscope fitted with a diode laser (Iris Medical, Inc.). The method of application and laser intensity were the same as that used to treat humans with retinal disorders (laser injuries of this extent to the optic nerve head and juxtapapillary nerve fiber layer cause monocular blindness). The laser did not affect the ocular media and caused no obvious discomfort. Atropine 1% and Cortisporin ointment were instilled on the conjunctiva of both eyes. The animals were awakened and returned to their home cages.

BDA injection

Three days after the laser procedure, the animals were re-sedated with i.m. ketamine and atropine. Mask induction of deeper anesthesia was achieved using isoflurane 3–5%. An intravenous line was inserted for administration of isotonic fluids (dextrose 5% in lactated Ringer's solution). To maintain anesthesia, a tracheal cannula was placed for inhalation of isoflurane 1–2%. Expired CO_2 was maintained between 4.5 and 5.5% and temperature was maintained at 37.5–38.0°C.

Using standard aseptic technique, the scalp was incised in the midsagittal plane and on each side, six to eight 3-mm-diameter burr holes were drilled in the skull overlying the operculum of the right and left V1. The holes were arranged in a grid-like pattern spaced ~ 0.75 cm apart, extending 1.5–2 cm anterior to the occipital ridge and bordering the midsagittal suture medially. Using a micromanipulator, glass micropipettes (tip diameter

15–20 μm) filled with 10% BDA (10,000 molecular weight, Molecular Probe, Eugene, OR) in 0.01 M phosphate buffer (pH 7.25) were lowered into the cortex through small slits in the dura to a depth of 0.6–0.8 mm. Small volumes (~10–50 nl) of BDA were injected by applying brief pulses (5–10 msec) of pressurized air (40 psi) to the back of the pipette (Picospritzer, General Valve, Inc.). After injection of the desired volume, pipettes were left in place for 1 minute. The pipettes were withdrawn, and the burr holes were irrigated copiously with sterile saline. The scalp was sutured closed. Both pupils were dilated with atropine 1%, and Cortisporin ointment was applied to the scalp wound. The animals were awakened and returned to their home cages. Postoperative analgesia was administered for 72 hours (buprenorphine i.m. 0.01 mg/kg every 8 hours).

Euthanasia and perfusion

Three days after tracer injections (a total of 7 days after laser deafferentation), the animals were re-anesthetized using ketamine. An overdose of sodium pentobarbital (120 mg/kg i.m.) was given. After pronounced slowing of the electrocardiogram was evident, the chest was opened to expose the heart. A cannula was inserted in the left ventricle, and 400 ml of a solution containing 2.6% paraformaldehyde, 0.1 M lysine-HCl, 0.8% $NaIO_4$, and 0.8% iodoacetic acid, pH 7.4 (modified PLP fixative of McLean and Nakane, 1974) was infused by a pump. The brain was then removed from the cranium and post-fixed in the same fixative for 2 hours. The skull was preserved for examination of extraocular muscles.

Orbital examination

Boothe and colleagues (1990) reported anomalies of the accessory lateral rectus (ALR) muscle in two *Macaca nemestrina* with naturally occurring esotropia (humans do not have an ALR). In one monkey, the ALR was absent but the lateral rectus muscle itself was larger than normal. In the other animal, the ALR was smaller than normal.

Analysis of the extraocular muscles and orbital pulleys in the *M. mulatta* and *M. nemestrina* of the current report, using serial sections of embedded whole orbits (Kono et al., 2002), revealed no lateral rectus anomalies (J.L. Demer and L. Tychsen, unpublished observations).

Brain sectioning

Opercular striate cortex and part of V2 was removed by cutting along the fundus of the lunate and inferior occipital sulci across the bottom of the internal calcarine sulcus. The resulting sheet of folded cortex was flattened by gentle pressure between glass slides. The tissue was post-fixed for an additional 1–2 hours in PLP fixative and equilibrated in 0.1 M phosphate-buffered 30% sucrose at 4°C. The tissue sheets were frozen rapidly on dry ice and sectioned at 40 μm on a freezing microtome in a plane parallel to the pial surface. Sections were collected in 0.1 M phosphate buffer, and alternate slices were stained for BDA, CO, and Nissl substance.

BDA histochemistry

For visualization of transported BDA, sections were first treated with 0.4% Triton X-100 and then incubated overnight at 4°C in a solution containing avidin–biotin–HRP complexes (Vectastain Elite Kit). After several rinses in 0.1 M phosphate buffer, BDA was visualized by reacting HRP with 0.05% diaminobenzidine (DAB) and 0.05% hydrogen peroxide. The reaction product was intensified with $AgNO_3$ and $HAuCl_4$ (Jiang et al., 1993). Sections were mounted on gelatinized slides, air-dried, dehydrated, cleared, and cover-slipped with DPX.

CO histochemistry

Differences in metabolic activity between ODCs were revealed by CO histochemistry using the staining protocol of Tootell and colleagues (1988). CO-stained sections were mounted and cover-slipped as described for BDA-stained tissue.

Analysis of BDA-labeled projections

Injection sites chosen for analysis were verified to be nonoverlapping and separated by a distance exceeding 5 mm (10 ODC widths). The centers of injection sites (uptake zones) were readily identified by a spot of dense brown BDA staining. The injection centers were 200–300 μm in diameter and, thus, smaller than the average width (~500 μm) of ODCs. Confidence in the small size of the uptake zone was derived from analysis of lateral geniculate nucleus (LGN) sections labeled retrogradely. Representative V1 injections, centered in an ODC, produced LGN labeling: (1) in LGN lamina corresponding to one eye and (2) spanning a narrow region (Malpeli and Baker, 1975) in each LGN lamina, corresponding to a retinotopic distance less than the width of an average opercular ODC (Adams and Horton, 2003).

To determine the exact location of the injection sites relative to ODC blobs and layers, BDA-stained sections were aligned with CO-stained sections (Fig. 1B) using blood vessels as reference marks. The relationships were determined and documented by superimposing digital images of BDA- and CO-stained sections, acquired using a Magnafire CCD camera (Optronics, Goleta, CA) and software from Soft Imaging System (Münster, Germany). The alignment served as a matrix for the analysis of BDA-labeled patches (clusters) composed of axons and boutons. Projection patches were identified as circumscribed regions of increased axonal branching. The boundaries of patches were determined by outlining regions of high bouton density viewed under the microscope. Post hoc analysis showed that, across these contour lines, the density of boutons changed by 80–90%. The territory occupied by CO blobs was determined from digital images by setting a 2:1 threshold between CO-poor and CO-rich regions. Territory within the boundary of the projection that did not also fall within the boundaries of CO-blobs was considered to be interblob territory. The strength of projections to CO-rich and CO-poor compartments was quantified for each injection as: the area of the BDA-labeled projections falling within a compartment (i.e., right eye ODC vs. left eye ODC, blob area vs. interblob area) / the total area of the BDA-labeled projections. Commitment of labeled patches to the same ocular dominance domain as the injected ODC was compared in normal vs. strabismic monkeys using Wilcoxon's rank sum test for unpaired samples of unequal size, with significance defined as $P < 0.05$.

Counting labeled boutons

BDA-labeled boutons were viewed with a 100× oil immersion lens and were identified as swellings ranging 0.5–1 μm in diameter (Fig. 8). For counting, 80- × 80-μm square fields were centered at BDA-labeled patches within successive left or right eye ODCs up to 4 mm to

TABLE 2. Strabismic Monkeys: Ocularity and CO-Blob Versus Interblob Assignment of BDA Injection Sites and Their Projections[1]

Monkey	Injection site[2]	Illustrated in figure	Center of injection site	Eccentricity[3]		% Area projection: Same eye ODC	Opposite eye ODC	Blob	Interblob
AR	L1	3A, B	Interblob	7.5°		84	16	12	88
AR	R1	2	Interblob	10°		77	23	39	61
AR	R3	3C, D	Interblob	7.5°		81	19	17	83
LA	L6	—	Interblob	7.5°		64	36	15	85
					Mean (SE)	76.5 (4.4)*	23.5 (4.4)	20.8 (6.1)	79.3 (6.1)*
LA	L7	3E, F	Blob	2.5°		69	31	45	55
AR	L2	—	Blob/interblob	10°		72	28	34	66
LA	L1	—	Blob/interblob	7.5°		66	34	34	66
					Mean (SE)	69.0 (3.0)	31.0 (3.0)	34.0	66.0

[1]Asterisks indicate $P < 0.05$, Wilcoxon rank sum test. CO, cytochrome oxidase; BDA, biotinylated dextran amine; ODC, ocular dominance column.
[2]R = right area V1; L = left area V1.
[3]Retinotopic distance from foveola (0° eccentricity).

either side of the injection center. An effort was made to sample all labeled patches. We estimate that this strategy encompassed > 90% of labeled patch territory. Counts of boutons were made from successive, focal planes separated by ~5 μm throughout the thickness of the section. To avoid double counting, the analysis only included boutons that were not contained in the preceding focal plane. Means of numerical densities of BDA-labeled boutons in strabismic monkeys were compared with mean densities of BDA-labeled boutons in normal monkeys using the *t* test for paired samples.

Measurement of neuronal soma size

Soma sizes were measured in Nissl-stained neurons of layer 2/3 and 4B residing within laser-deafferented and nondeafferented ODCs. The perimeter of individual neuronal somata was viewed at 1,200× magnification and was measured in the focal plane that contained the nucleolus. Mean cross-sectional areas for 30 neurons in each lamina were compared using the *t* test for paired samples.

RESULTS

Ocularity and specificity of labeled projections in strabismic monkeys

In each monkey, injections into opercular V1 produced excellent local axonal labeling. Approximately 40% of injections were confined to a single ODC and, therefore, suitable for analysis. Nine injections were made in strabismic monkey AR and eight in strabismic monkey LA (four of nine analyzed in AR and three of eight in LA). Each injection was centered in the middle of cortical gray matter (layer 4) and extended vertically to include supra- and infra-granular layers. The retinotopic maps of Van Essen et al. (1984), LeVay et al. (1985), and Tootell et al. (1988) served as a guide to estimate eccentricities, using the calcarine sulcus, optic disc representation, and V1/V2 borders as landmarks in reconstructions from serial sections (Tychsen and Burkhalter, 1997). The retinoptic location of the seven injection sites used for quantitative analysis in the two strabismic monkeys is listed in Table 2, along with assignment to a right or left eye ODC, and blob or interblob territory.

Figure 2A shows a representative BDA injection in a section through flattened V1 (layer 2/3) of strabismic monkey AR. Even at low magnification, BDA-labeled axons can be seen radiating in all directions and forming multiple dense terminal clusters at regular intervals. Figure 2B depicts an adjacent CO-stained section that traverses through layers 2/3 and 4C, revealing the familiar stripe pattern of layer 4C ODCs. The injection site (marked by white asterisk in Fig. 2A) was centered in a pale ODC representing the deafferented left eye. Figure 2C shows a section through layer 2/3 in which rows of CO-blobs are visible that lie in register with OD-stripes (Fig. 2B). A small injury caused by the injection pipette indicates that the BDA injection was centered in an interblob region. Although interblob vs. blob regions were readily identified, the borders of blobs were often not sharply definable. Thus, we acknowledge that, in this and the subsequent injections, we describe there may have been some blob involvement in what appeared to be a discrete interblob injection. Projections from this interblob site tended to terminate preferentially in other interblobs, with 61% of the labeled patches projecting to interblob territory (Table 2, second row).

The relationships of BDA-labeled projections to blobs, interblobs, and ODCs are illustrated with greater clarity in Figure 2D, which is an overlay of Figure 2A–C. The overlay reveals by qualitative inspection that the projections preferred to terminate in ODCs representing the same eye, which produced a "skipping" pattern of labeling when the sections were viewed at low power. Quantitative analysis revealed that 77% of the labeled projections for this injection occupied pale ODCs representing the same ocularity as the injected (left eye) ODC (Table 2, second row). The skipping pattern was observed in all of the injections in the strabismic monkeys and was independent of the location of the injection relative to blobs and interblobs.

Composite diagrams of two additional interblob injections in strabismic monkey AR are shown in Figure 3A–D. The injection site is marked by an asterisk, and BDA-labeled projection fields are depicted as dark patches. CO-rich ODCs of layer 4C are shown as gray stripes (Fig. 3A,C), and CO-blobs of layers 2/3 are shown as gray ovals (Fig. 3B,D). The projections in these injections, together with the injection of Figure 2, revealed a monocularly biased pattern of connectivity; 77–84% of the projections were to ocular dominance stripes representing the same eye as the injected ODC. In addition to showing a monocular bias, an interblob-to-interblob preference was also evident; 61–88% of projections from interblob injections landed in other interblob territory (Table 2, rows 1–3).

In the second strabismic monkey (LA), one of the three injections suitable for analysis was confined to interblob

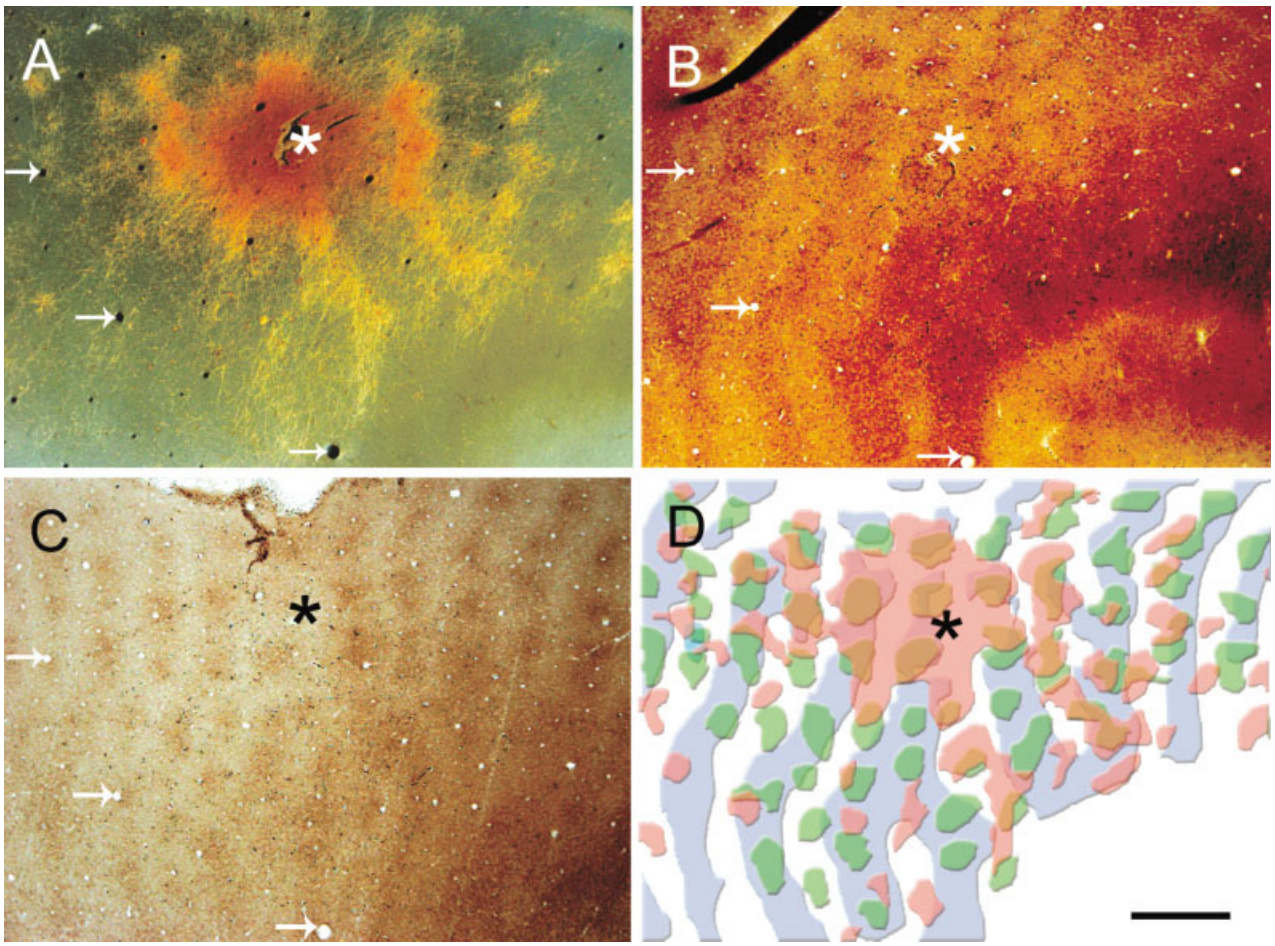

Fig. 2. **A:** Photomicrograph of biotinylated dextran amine (BDA) -labeled horizontal connections in layer 2/3 of flattened, opercular V1 at 10 degrees eccentricity of a strabismic monkey (AR). Patches of labeled axon terminals are embedded within a lattice-like arrangement of labeled axons and terminal branches emanating from the injection site (asterisk). Note the fluctuating ("skip") pattern of labeling, which was typical of the injections in strabismic monkeys. At higher power the skip pattern was verified to be due to greater numbers of axonal boutons in every other row of ocular dominance columns (ODCs). Arrows indicate blood vessels that were used as reference marks for aligning adjacent sections. **B:** Alternate cytochrome oxidase (CO) -stained section through layer 2/3 and 4C to reveal ODC-stripes. The BDA injection (asterisk) was centered just within a CO-pale ODC representing the left eye. **C:** Adjacent CO-stained section through layer 2/3 to reveal CO-blobs. The BDA injection (asterisk) was in an interblob region. **D:** Composite diagram of injection shown in A, B, and C made by overlay of adjacent BDA-labeled and CO-stained sections through layer 2/3 and 4C to reveal relationship of connections (red) to CO-blobs (green) and ODC-stripes (blue). Note two major findings: (1) the BDA was injected into a left eye ODC-stripe and labeled axons predominantly (77%) in other left eye ODCs; and (2) the BDA was injected into an interblob compartment and labeled axons predominantly in other interblob (61%) compartments. Scale bar = 1 mm in D (applies to A–D).

territory. Quantitative analysis of this injection showed a similar but less striking monocular bias, with 64% of projections to ODCs of the same ocularity as the injected ODC. The projections from this injection also conformed strongly to an interblob-to-interblob rule of connectivity in that 85% of projections were confined to interblob territory (Table 2, fourth row).

One injection in monkey LA was confined to blob territory (Fig. 3E,F). A monocular bias was evident, with 64% of projections to ODCs of like ocularity. A blob-to-blob connectivity preference, however, was not evident: 45% of projections were to blob territory and 55% to interblob (Table 2, fifth row). The remaining injections (Table 2, last two rows) in the two strabismic monkeys straddled blob/interblob regions and showed a moderate preference favoring projection (66%) to other interblob regions. Both of these blob/interblob injections revealed a monocular bias, with 66–72% of projections to ODCs of the same ocularity as the injected ODC.

Ocularity and specificity of labeled projections in normal monkeys

To help interpret the results of patchy axonal labeling in V1 of the strabismic monkeys, we used the same methods to analyze projection patches in normal macaques with the goal of answering two questions: (1) Do strabismic monkeys, when compared with normal monkeys, have a relative paucity of binocular connections? And (2) if so, is the paucity between interblob compartments, blob compartments, or both?

Figure 4A shows a BDA-labeled section through layer 2/3 of normal monkey ER. The qualitative difference in the

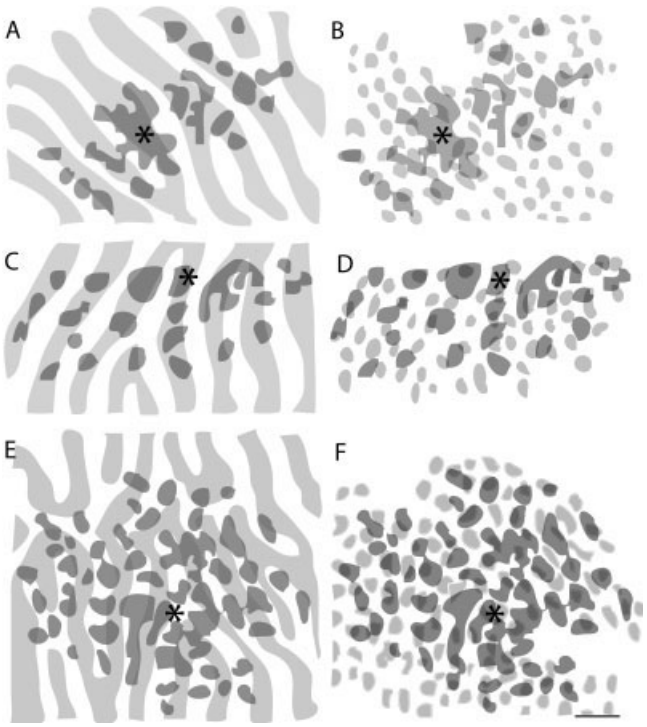

Fig. 3. Composite diagrams of biotinylated dextran amine (BDA)-labeled and cytochrome oxidase (CO) -stained sections through layers 2/3 of opercular V1 showing three injection sites in two strabismic monkeys. In all panel, BDA-labeled connections are indicated by dark patches. In A, C, and E, light gray stripes represent right eye ocular dominance columns (ODCs), whereas white stripes represent left eye ODCs. In B, D, and F, blobs are represented as light gray ovals. **A:** An injection (asterisk) in the left opercular V1 at 7.5 degrees eccentricity of monkey AR. BDA injection was made within a right eye ODC-stripe, and labeled axons predominantly (84%) in other right eye ODCs. **B:** Same injection as A, showing BDA injection was made into an interblob region and label was transported predominantly (88%) to other interblob regions. **C:** An injection (asterisk) in the right opercular V1 at 7.5 degrees eccentricity of monkey AR. BDA injection was made within a right eye ODC-stripe and was transported predominantly (81%) to other right eye ODCs. **D:** Same injection as C, showing the BDA injection was made into an interblob region, and the label was transported predominantly (83%) to other interblob regions. **E:** An injection (asterisk) in the left opercular V1 at 2.5 degrees eccentricity of monkey LA. BDA injection was made within a left eye ODC-stripe and was transported predominantly (69%) to other left eye ODCs. **F:** Same injection as E, showing BDA label was injected into a CO-blob and was transported to both CO-blobs (45%) and interblobs (55%). Scale bar = 1 mm.

pattern of connectivity between a strabismic and normal animal can be observed by comparing the pattern of BDA-labeled patches in Figure 4A with that of Figure 2A. The "skipping" pattern of labeling in strabismic V1 differed strikingly from the labeling pattern in normal V1, which has been termed a "sunburst" (Livingstone and Hubel, 1984b). At higher power, the sunburst pattern was verified to be due to a systematic decrease in the numbers of labeled axon terminations as a function of distance from the center of the injection. Figure 4B is an adjacent section through layer 4C stained by using CO to reveal ODC stripes. The injection (asterisk) was centered in a CO-dark ODC, representing the right (nonlasered) eye. Figure 4C is a CO-stained section through layer 2/3, showing that the BDA injection was centered in an interblob region. Figure 4D is an overlay of Figure 4A–C; the projections from the site of the injection showed a strong preference for connection to interblob compartments (74%) but a weaker preference (61%) for connection to ODCs of like-ocularity (Table 3, first row).

Labeling of connections from a second interblob injection in normal monkey ER is shown in the composite diagram of Figure 5A,B. For this injection, 58% of projections were to ODCs of the same ocularity and 65% of projections were to other interblob regions. Qualitatively and quantitatively similar results were obtained for the four other interblob compartment injections in the normal monkeys (Table 3, rows 1–6): 58–61% of labeled projections terminated in ODCs of the same ocularity (i.e., a small monocular bias) and 62–76% of projections terminated in interblob regions (i.e., a moderate interblob-to-interblob connection specificity).

The results of a representative blob compartment injection in normal monkey ER are shown in the composite diagrams of Figure 5C,D. Blob compartment injections (n = 3) in this normal animal showed a variable tendency toward monocular connectivity: 56–73% of projections were to ODCs of like ocularity. Moderate blob-to-blob connection specificity was evident also, with 53–76% of projections terminating in other blob compartments (Table 3, rows 7–9). The remaining injections (n = 2, Table 3, last two rows) in normal monkey ME straddled blob/interblob regions and, taken together, showed no consistent ocularity bias and a minimal preference (55.5%) favoring interblob projection.

The bar graphs of Figures 6 and 7 summarize the results of patchy labeling in the four monkeys. Figure 6 illustrates with greater clarity how the ocularity of horizontal V1 connections tended to differ in strabismic vs. normal animals as a function of injection compartment. For injections into interblob compartments, the percentage of monocular projections was greatest in strabismic monkeys and least in normal monkey, which is to say the difference in binocular connectivity between strabismic and normal monkeys was most pronounced for connections between interblob compartments ($P < 0.01$; Wilcoxon rank sum test). The difference in binocular connectivity between strabismic and normal was less pronounced for mixed interblob/blob injections, and minimal for blob injections (both nonsignificant at 5%, rank sum), i.e., for blob injections, the strabismic and the normal monkeys showed a similar monocular bias.

Figure 7 plots the commitment of labeled patches to the same compartment as the injection site, for each blob and interblob injection in each animal (the four mixed blob/interblob injections are not shown). Of these 14 injections, 11 (79%) were characterized by a >60% commitment to the same CO-compartment ($P < 0.01$, rank sum). Of the three other injections, two (14%) were blob injections in normal monkey that measured a commitment > 50%, and one (7%)—the single exception—a blob injection in strabismic monkey (LA L7) showed <50% commitment (variability in commitment of this degree or greater for individual blob injections was also reported by Yoshioka et al., 1996).

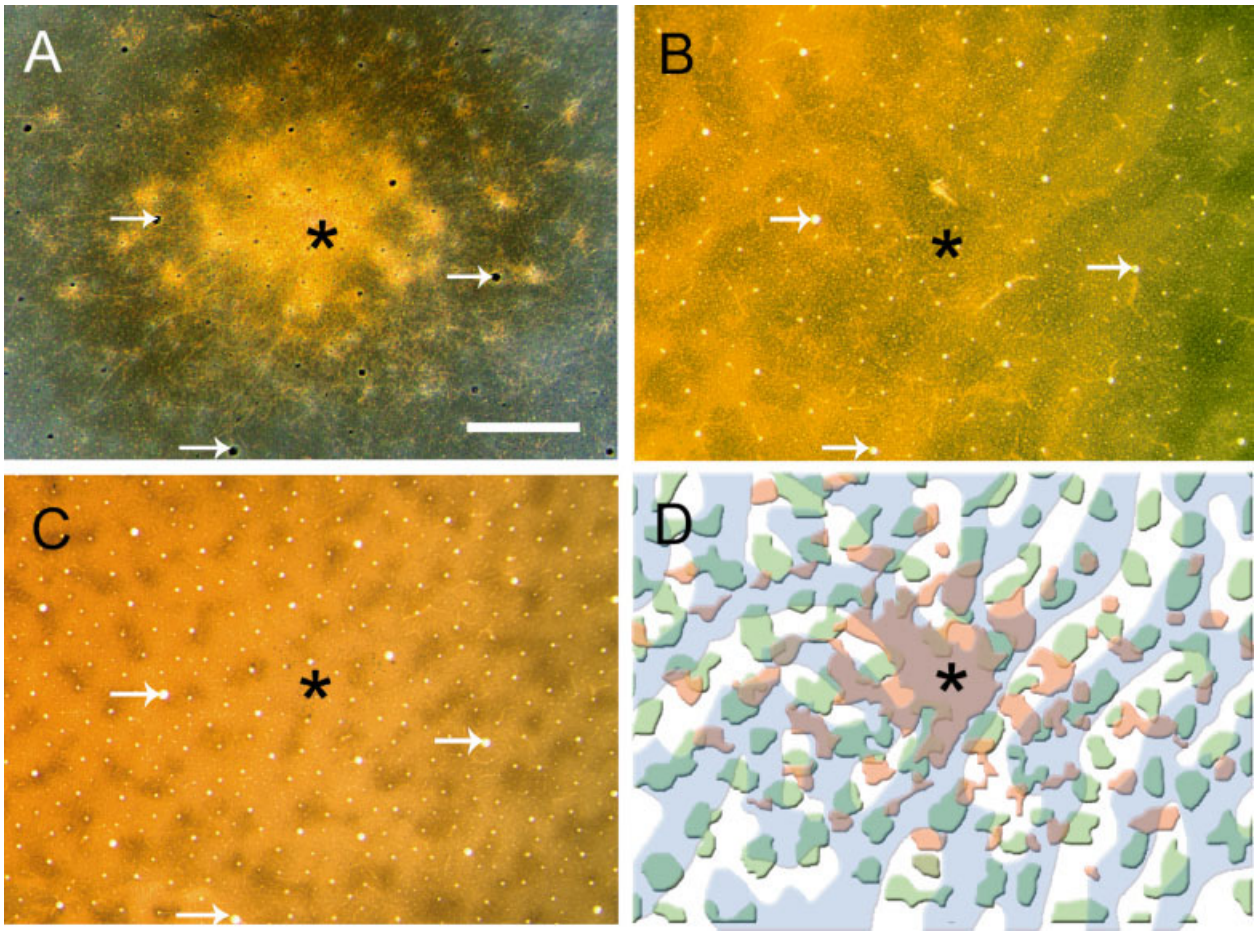

Fig. 4. **A:** Photomicrograph of biotinylated dextran amine (BDA) -labeled horizontal connections in layer 2/3 of flattened, opercular V1 at 2.5 degrees eccentricity of a normal monkey (ER). Note the "sunburst" pattern of anterograde labeling emanating from the site of injection (asterisk), which was typical of the injections in normal monkeys. Arrows indicate blood vessels that were used as reference marks to align adjacent sections. **B:** Alternate cytochrome oxidase (CO) -stained section through layer 4C to reveal ocular dominance column (ODC) -stripes. The BDA injection (asterisk) was centered within a CO-dark ODC representing the right eye. **C:** Adjacent CO-stained section through layer 2/3 to reveal CO-blobs. The BDA injection marked by the asterisk was seen in an interblob region. **D:** Composite diagram of injection shown in A, B, and C made by overlay of adjacent BDA-labeled and CO-stained sections through layer 2/3 and 4C to reveal relationship of connections (red) to CO-blobs (green) and ODC-stripes (blue). Note that the BDA was injected into an interblob region and was anterogradely transported predominantly (74%) to other interblob regions. Scale bar = 1 mm in A (applies to A–D).

Anisotropy of horizontal connections and pattern of ODCs

BDA-labeled patches in V1 of both strabismic and normal animals tended to be distributed in an elliptical shape (Figs. 2–5). The ellipse center was the site of injection and the long axis was oriented orthogonal to the local boundaries of ODCs (Malach et al., 1993; Yoshioka et al., 1996). Thus, near the V1/V2 border the connections were elongated parallel to the vertical meridian of the visual field. Near the horizontal meridian, they were elongated oblique to the meridian (Van Essen et al., 1984). The aspect ratio of long/short axes ranged from 1.6 to 2.3 in the strabismic monkeys, and from 1.2 to 2.2 in the normal monkeys. The ratio in all of the animals was similar to the anisotropy of visual field magnification (Van Essen et al., 1984). When projected onto visual space, the ellipses approximated a circle.

The overall pattern of ODC stripes in layer 4C of strabismic animals appeared normal, with stripes abutting the vertical meridian orthogonally at the V1/V2 border, and arranged elsewhere roughly orthogonal to an imaginary ray emanating from the point of fixation (Hubel and Wiesel, 1977; LeVay et al., 1985). The exceptions to this were the horizontal meridian, where they tended to run parallel to the meridian, and near zero eccentricity, where the pattern was irregular, as in normal animals. The (400–500 μm) width of ODCs in opercular cortex of the strabismic monkeys was comparable to that measured in normal macaques and in macaques who have infantile-onset (Tychsen and Burkhalter, 1997; Fenstemaker et al., 2001) or adult-onset strabismus (Horton et al., 1999).

Counts of terminal boutons in layer 2/3 and 4B

Judging binocular connections based on the extent of connection, relative to ocular domains, might be misleading, because a reduction in the extent of innervation might

TABLE 3. Normal Monkeys: Ocularity and CO-Blob Versus Interblob Assignment of BDA Injection Sites and Their Projections[1]

Monkey	Injection site[2]	Illustrated in figure	Center of injection site	Eccentricity[3]		% Area projection: Same eye ODC	Opposite eye ODC	Blob	Interblob
ER	L3	4	Interblob	2.5°		61	39	26	74
ER	L1	5A, B	Interblob	5°		58	42	35	65
ER	R2	—	Interblob	7.5°		43	57	24	76
ER	R3	—	Interblob	7.5°		56	44	26	74
ME	L2	—	Interblob	5°		57	43	38	62
ME	R2	—	Interblob	5°		58	42	32	68
					Mean (SE)	55.5 (3.1)	44.5 (3.1)	30.2 (2.4)	69.8 (2.4)*
ER	L2	5C, D	Blob	2.5°		65	35	76	24
ER	L4	—	Blob	3.75°		73	27	53	47
ER	L5	—	Blob	10°		56	44	58	42
					Mean (SE)	64.7 (5.0)	35.3 (5.0)	62.3 (7.0)	37.7 (7.0)
ME	R3	—	Blob/interblob	7.5°		46	54	41	59
ME	L1	—	Blob/interblob	7.5°		62	38	48	52
					Mean (SE)	54.0 (8.0)	46.0 (8.0)	44.5 (3.5)	55.5 (3.5)

[1]Asterisks indicate $P < 0.05$, Wilcoxon rank sum test. CO, cytochrome oxidase; BDA, biotinylated dextramine; ODC, ocular dominance column.
[2]R, right area V1; L, left area V1.
[3]Retinotopic distance from foveola (0° eccentricity).

be offset by an increase in the innervation strength. To provide a direct measurement of the strength of connection, we determined the numerical density of axonal boutons (Fig. 8) for BDA-labeled patches layers 2/3 and 4B. To rule out contamination by collateral projections of retrogradely labeled neurons, injections that produced back-labeled neurons were excluded from the analysis.

Figure 9A shows mean terminal bouton densities (±SD) within layer 2/3 in the strabismic animals. The density of labeled boutons in same-eye ODCs (lighter bars) exceeded the density in opposite-eye ODCs (darker bars) by 53–60% (paired t test, $P < 0.01$; comparing ODC pairs: column 0 to column 1, 2 to 3, 4 to 5). In normal monkeys (Fig. 9B), the differences for same-eye vs. opposite-eye mean bouton densities were 0–27% ($P > 0.30$; comparing each successive ODC pair). Mean densities for several adjacent ODC pairs differed by less than 5% in the normal monkeys, including those of layer 4B. In both strabismic and normal animals, bouton density four-or-more ODC widths from the injection center was approximately half that at the injection center and tended to decrease as a function of distance from the center.

The paucity of boutons in opposite-eye ODCs was equally severe in layer 4B of the strabismic animals (Fig. 9C). Bouton density in same-eye columns exceeded bouton density in opposite-eye columns by 57–66% ($P < 0.01$; comparing each successive ODC pair). In layer 4B of the normal animals (Fig. 9D), the mean bouton differences were 0–18% ($P > 0.60$; comparing each successive ODC pair).

Size of pyramidal neurons and interbouton distance

Because the axons of pyramidal neurons in the strabismic monkeys formed fewer boutons in opposite-eye ODCs, one might expect the size of neuronal somata to be smaller in the strabismic animals. It is also possible, although unlikely, that neurons in V1 of the strabismic monkeys might have responded more severely by means of transsynaptic degeneration to laser deafferentation of one eye. If this were the case, one would expect to see disproportionate shrinkage of the somata receiving input from the deafferented eye. To rule out these possibilities, we measured the average size of neuronal somata in layers 2/3 and 4B in strabismic and control animals. No differences were found; mean somata area of deprived-ODCs in strabismic V1 was 166.2 ± 22 μm^2, compared with 159.9 ± 28 μm^2 in normal controls (t test; $P > 0.40$). Inspection of synaptic bouton distribution along axons revealed no marked variation in interbouton distance in the strabismic monkeys. Mean interbouton distances were on average 5–10 μm in all animals (Amir et al., 1993).

DISCUSSION

The main result of our experiments is summarized in the schematic of Figure 10. It shows that in V1 of naturally strabismic monkeys, long-range horizontal connections preferentially link ODCs belonging to the same eye. The preference for monocular connectivity in the strabismic monkeys was similar for interblob and blob-compartment neurons. In contrast, V1 in normal monkeys had abundant connections between ODCs representing the right and left eyes, but this finding was most pronounced for interblob neurons and less pronounced for blob neurons. The reduction of binocular connections in strabismic V1 was revealed by analysis of the proportion of the projection that occupies the opposite eye compartment (21% average reduction, Fig. 6) and confirmed by determining bouton density (~50% reduction overall, Fig. 9A,C). The connectivity deficit was evident equally in layers 2/3 and 4B, which contain neurons in the pathways that mediate binocular perception and ocular motor functions, including disparity sensitivity, motion sensitivity, eye alignment, and eye movement (Van Essen, 1985; Chino et al., 1997; Kumagami et al., 2000; Cumming and DeAngelis, 2001). All of these sensorimotor functions have been shown to be impaired in humans and monkeys with infantile strabismus (Tychsen, 1999). The paucity of binocular connections in the strabismic monkeys help explain their perceptual and ocular motor deficits.

Technical considerations

The interpretation of our results depended on our ability to confine and assign BDA injections to single ODCs. Our results show that the BDA injection sites were 200–300 μm in diameter and, thus, smaller than the (400–500 μm) width of ODCs (Tychsen and Burkhalter, 1997). When centered in an ODC, the injections produced retrograde labeling of LGN lamina corresponding to that eye

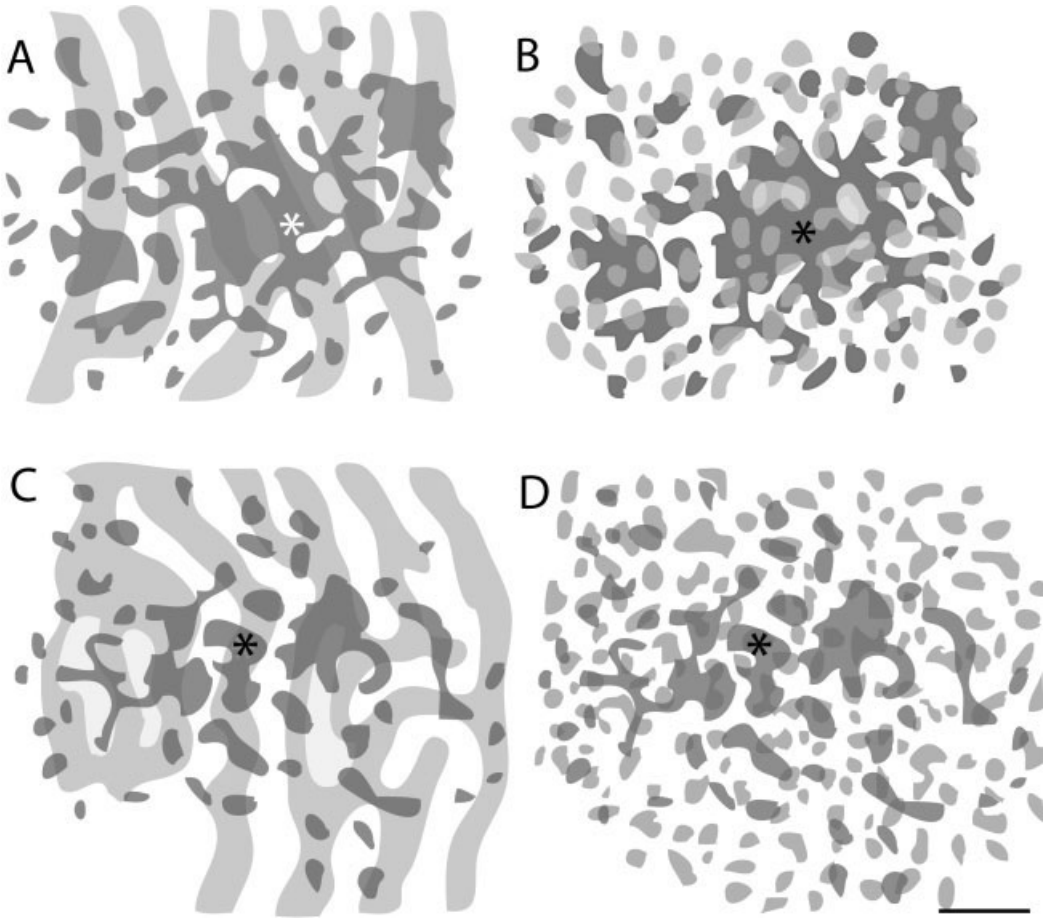

Fig. 5. Composite diagrams of biotinylated dextran amine (BDA) -labeled and cytochrome oxidase (CO) -stained sections through layers 2/3 of opercular V1 showing two other injection sites in a normal monkey (ER). In all panels, BDA-labeled connections are indicated by dark patches. In A and C, light gray stripes represent right eye ocular dominance columns (ODCs), whereas white stripes represent left eye ODCs. In B and D, blobs are represented as light gray ovals. **A:** An injection (asterisk) in the left opercular V1 at 5 degrees eccentricity. BDA injection was made within a right eye ODC-stripe and was transported fairly evenly to other right eye (58%) and left eye (42%) ODCs. **B:** Same injection as A, showing the BDA injection was made into an interblob region, and 65% of the label was transported to other interblob regions. **C:** An injection (asterisk) in the left opercular V1 at 2.5 degrees eccentricity. BDA injection was made within a right eye ODC-stripe and was transported fairly evenly to other right eye (65%) and left eye (35%) ODCs. **D:** Same injection as C, showing the BDA injection was made into a blob region, and the label was transported predominantly (76%) to other blob regions. Scale bar = 1 mm.

only. The technique of making multiple "blind" injections of BDA in a grid-like manner across V1 is less elegant than a direct approach using optical imaging (Malach et al., 1993; Yoshioka et al., 1996). However, with a success rate ~40% for injecting single ODCs it provides a simple, workable approach with several advantages. Studies that have used optical imaging to assess ocular dominance domains lumped labeled patches into right eye or left eye territory when 67% of the label fell within a single ODC (Malach et al., 1993; Yoshioka et al., 1996). The method we used avoided lumping in assigning projection patches to compartments, and relied on exact measurements of the area of overlap between projections, ODCs, blobs, and interblobs. This method is more precise and affords the resolution necessary to detect modifications of binocular connectivity that are ≤33%. Determining the borders of projection patches using any current methodology does require, inevitably, some interpretation. The most common error may be overestimation of patch size, due to the inclusion of unbranched fibers when judging the outer boundary of an individual patch. To help ensure that the analysis was rigorous, we took the quantification a step further and counted labeled boutons in right and left eye domains. Bouton counting confirmed the results of patch analysis and showed an unequivocal reduction of binocular synapses within the strabismic animals' V1.

BDA provided as detailed a delineation of axonal patches in macaque V1 as provided by HRP (Rockland and Lund, 1983; Livingstone and Hubel, 1984a,b) biocytin (Amir et al., 1993; Lund et al., 1993; Malach et al., 1993) or cholera toxin subunit B (Angelucci et al., 2002). Retrograde labeling was rare. When present, the few back-labeled neurons were distributed equally in all compartments, which rules out that differences in bouton density were due to selective labeling of collaterals of retrogradely labeled neurons. The paucity of connections in the strabismic animals cannot be explained as reduced active transport of BDA by neurons within laser-deafferented

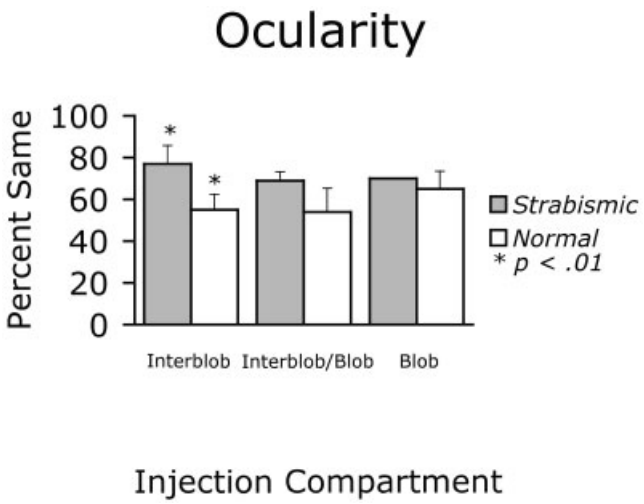

Fig. 6. Mean percentage of the connection area in ocular dominance columns (ODCs) of the same ocularity as the injected ODC, strabismic vs. normal V1. For interblob compartment injections, the monocular bias in strabismic monkeys (77%) was significantly greater than in normal monkeys (56%; Wilcoxon's rank sum test). Each column represents the average for all injections into interblob, blob, and mixed compartments.

ODCs. In both the normal and strabismic monkeys, the average size of neurons was equal in CO-rich and poor ODCs, BDA was transported from CO-rich and poor ODCs alike an average 3–5 mm (6–10 ODC widths), and we found no difference in the number of boutons labeled within a given animal when comparing a right eye ODC injection to a left eye ODC injection.

Blob and interblob compartment specificity

Livingstone and Hubel (Livingstone and Hubel, 1984a) first described a CO-compartment specificity of long-range horizontal connections in macaque V1. Based on qualitative analysis of HRP injections, they concluded that projections from CO-blobs targeted other blobs, and interblobs were connected to other interblobs (Livingstone and Hubel, 1984a). Lund et al. (1993) and Malach et al. (1993) used qualitative analysis of biocytin injections to reach the same conclusion: CO-blobs appeared to be selectively interconnected. A subsequent study by Lund's group, using quantitative analysis of biocytin injections, revealed that the commitment of patchy connections to the same CO-compartment was in fact reasonably strong (71%) but far from absolute (Yoshioka et al., 1996). Quantitative analysis of the BDA injections in our normal monkeys supports the "reasonably-strong-but-not-absolute" rule that appears to apply for connections between CO-compartments. We found that the commitment to the same CO-compartment was on average 70% for interblob injections and 62% for blobs (Fig. 6). The 62% commitment of blob connections is particularly impressive given that only 21% of layer 2/3 territory in macaque V1 is devoted to blobs (Yoshioka et al., 1996). That blob-connection specificity (62%) exceeds blob territory (21%) by a factor of almost three makes it unlikely that our results, or those of these previous studies, could have arisen by chance from a random distribution of labeled patches. Our findings support the dictum that, while connectivity between similar compartments predominates, a rich intermingling of information takes place between the functional streams that flow within and from V1 to the pathways of extrastriate cortex (Yoshioka et al., 1996; Callaway, 1998; Sincich and Horton, 2002).

Ocularity of blob and interblob compartments

Single unit recordings from layers 2/3 in V1 of normal macaque (Livingstone and Hubel, 1984a) have shown that a major proportion of interblob neurons respond in balanced binocular manner (i.e., 41% fall into ocular dominance groups 3–5). The anatomy of horizontal connections in V1 of our normal animals is consistent with this physiology; the interblob injections labeled same-eye vs. opposite-eye ODCs in quasibalanced manner (56% vs. 44%, Fig. 6). Single unit recordings within CO-blobs have shown more pronounced monocular specificity (Livingstone and Hubel, 1984a; Ts'o and Gilbert, 1988) in that only 15% of blob neurons fall into (binocular) ocular dominance groups 3–5. In our normal monkeys, a monocular bias for blob connections was likewise evident: blob injections produced preferential labeling of same-eye as opposed to opposite-eye ODCs in a proportions of 65% and 35%, respectively.

Studies that have used optical imaging to assess ocular dominance have produced, with respect to the monocular specificity of connections in normal macaques, mixed results (Malach et al., 1993; Yoshioka et al., 1996). The ocularity study by Malach et al. did not include an analysis of CO-compartments. But they did report that biocytin injections into "monocular regions" vs. "binocular regions" produced labeling highly specific (87–90%) for other monocular or binocular regions, respectively. Yoshioka et al., on the other hand, reported that only 54% of biocytin-labeled patches fell into the same optically imaged OD category as the injection site, with no clear difference

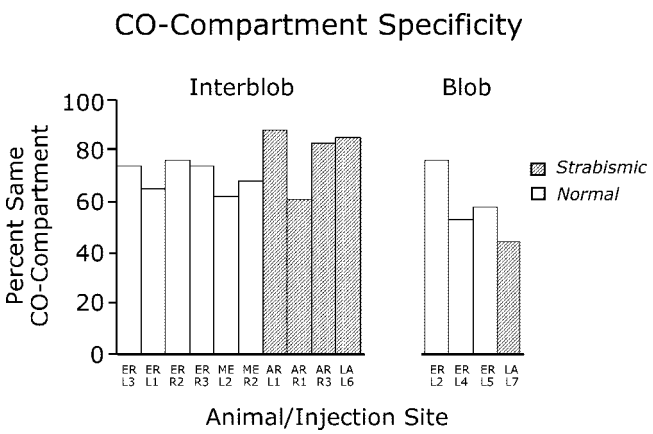

Fig. 7. Percentage of connection area in same cytochrome oxidase (CO) -compartment as the injected compartment, interblob vs. blob territory injections in normal and strabismic V1. All interblob connections (n = 10 injections) showed commitment >60% to the same compartment. Three-of-four blob injections showed commitment >50% to the same compartment. Each column represents an individual injection with animals and sites listed in Tables 2 and 3. Mixed blob/interblob injections (n = 4) not shown.

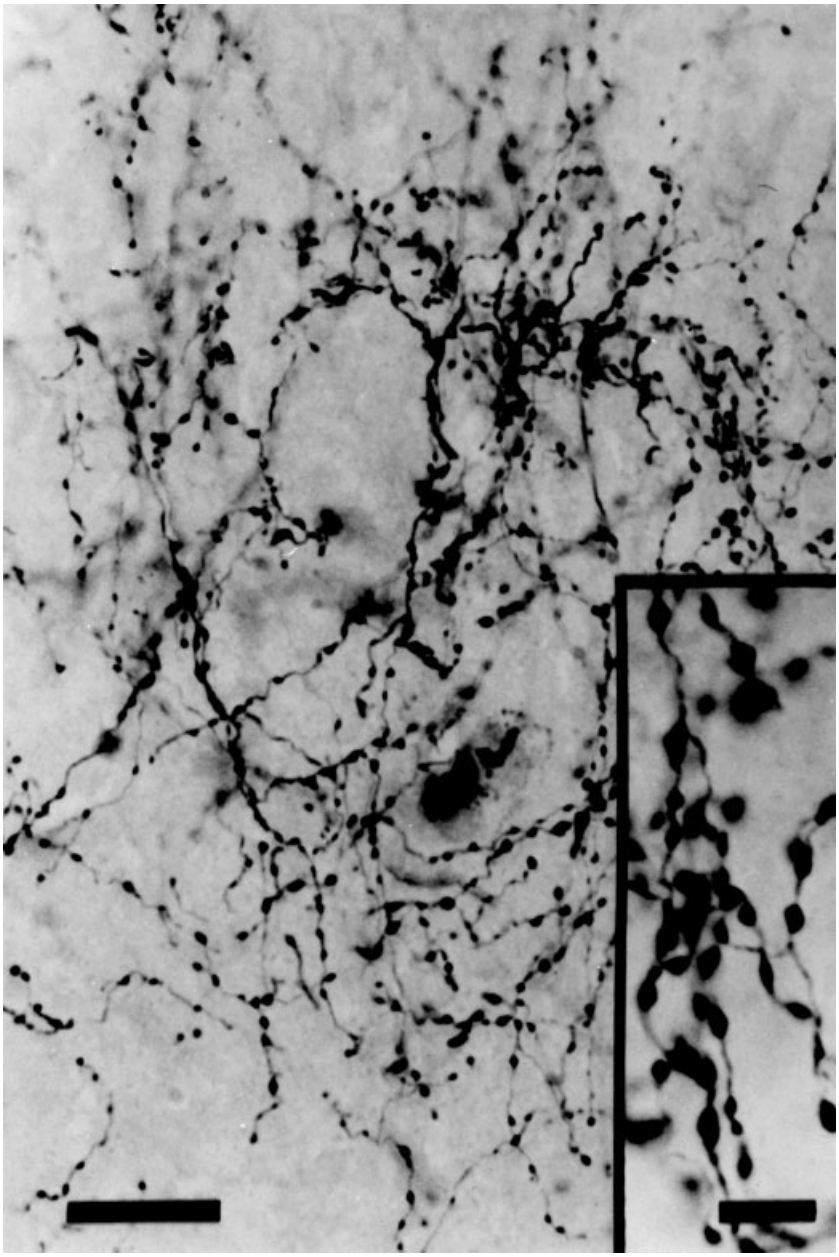

Fig. 8. High power photomicrograph of biotinylated dextran amine–labeled axons and boutons in layer 2/3 of V1 of strabismic monkey. Scale bars = 40 μm; 10 μm in inset.

between injections into CO-blob vs. interblob compartments. It is possible that the results of the current study differ from those of the previous studies because of the greater precision that can be achieved in alignment of CO-labeled ODCs with blobs, interblobs, and projections, as opposed to mapping an optical signal to the anatomical substrate. Experiments comparing these methods directly should help resolve the apparent discrepancies.

Binocular connections in infantile strabismus: nurture and nature

Our findings in strabismic monkey help to define the role of visual experience in the development of ODCs and their connections within primary visual cortex (Katz and Crowley, 2002). The current work and earlier work from our laboratory and others indicate that many aspects of V1 development in monkey are innate and largely unperturbed by strabismus during the critical period. The division of primary cortex into distinct layers and columns (LeVay et al., 1978; Crawford and Von Noorden, 1979; Wiesel, 1982), the spacing of ODCs and CO-blobs (Tychsen and Burkhalter, 1997; Fenstemaker et al., 2001), the density of neurons within columns (Fenstemaker et al., 2001), and the length of horizontal axonal projections (Wong et al., 1998; Tychsen et al., 2000) appear to be largely unaffected by early-onset strabismus. The results of the current study also indicate that the size of neuronal somata and the anisotropy of axonal projections develop independent of correlated binocular activity in adjacent ODCs. Subtle changes in the cytoarchitecture of ODCs have been

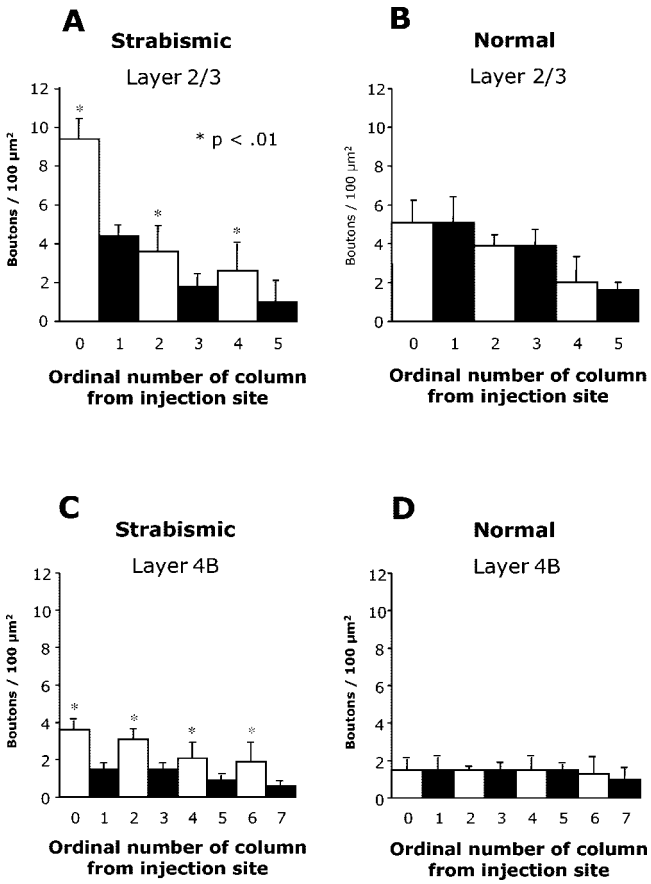

Fig. 9. Density of axonal boutons (mean ± SD) in right and left eye ocular dominance columns (ODCs) of V1 after injection into a right or left eye ODC, strabismic vs. normal monkey. The injected ODC is at zero on the X axis. **A:** Strabismic, layer 2/3: 53–60% greater density of boutons in same eye (gray) vs. opposite eye (black) ODCs after injection into a right or left eye ODC (t test; asterisks indicate $P < 0.01$ comparing ODC 0 with ODC 1; 2 to 3; 4 to 5). **B:** Normal, layer 2/3: less than a 27% difference in bouton density in same eye (open bars) vs. opposite eye (filled bars) ODCs after injection into a right or left eye ODC ($P > 0.30$, comparing successive ODC pairs). **C:** Strabismic, layer 4B: 57–66% greater bouton density in same eye (open bars) vs. opposite eye (filled bar) ODCs after injection into a right or left eye ODC (asterisks indicate $P < 0.01$). **D:** Normal, layer 4B: less than a 18% difference in bouton density in same eye (open bars) vs. opposite eye (filled bars) ODCs after injection into a left eye ODC ($P > 0.60$).

observed in macaques with early-onset strabismus. In layer 4C, alterations in CO staining, as well as calbindin and neurofilament protein labeling, are most apparent at the borders of ODCs and may prove to be markers for loss of binocular neurons in these zone (Fenstemaker et al., 2001).

The ~50% reduction of binocular axonal boutons in our strabismic monkeys was most likely the result of abnormal visual experience in infancy. Misalignment of the visual axes would have desynchronized activity in right and left eye ODCs and led to excessive pruning of binocular connections during the critical period (Hebb, 1949; Hubel and Wiesel, 1965; Van Sluyters and Levitt, 1980; Lowel and Singer, 1992; Trachtenberg and Stryker, 2001). Monkeys reared with experimentally induced, alternating esotropia have very few neurons in V1 that can be driven binocularly (LeVay et al., 1978; Crawford and Von Noorden, 1979; Wiesel, 1982). Kittens reared with artificial exotropia are known to have desynchronized activity in opposite-eye ODCs and a paucity of binocular connections (Lowel and Singer, 1992; Roelfsema et al., 1994; Trachtenberg and Stryker, 2001). If strabismus is induced in kittens at the height of the critical period, the loss of patchy binocular projections and axonal boutons takes place within 2 days (Trachtenberg and Stryker, 2001). The time course for loss of binocular connections in strabismic infant primates is unknown but can be inferred from behavioral work to be within a matter of weeks in monkey and months in human (Birch et al., 2000; Wong et al., 2003). Repair of experimental strabismus in infant monkey by age 3 weeks restores normal binocular sensory and motor behaviors but delay of repair until age 12 weeks causes permanent impairment (Wong et al., 2003). Repair of strabismus in human infants, within 2–3 months of onset, has been reported to produce good-to-excellent eye alignment and restoration of fine stereoscopic vision (Wright et al., 1994; Birch et al., 2000). Repair delayed beyond age 12 months is associated with substantially poorer binocular function.

It is important to note that the strabismic monkeys we studied possessed all of the behavioral features of human infants with strabismus. They developed natural alternating, nonparalytic esotropia and, like many strabismic human infants, had normal monocular visual acuity in each eye (Kiorpes and Boothe, 1981; Tychsen et al., 2000). The lack of horizontal connections between opposite-eye ODCs would not be expected to impair monocular spatial vision,

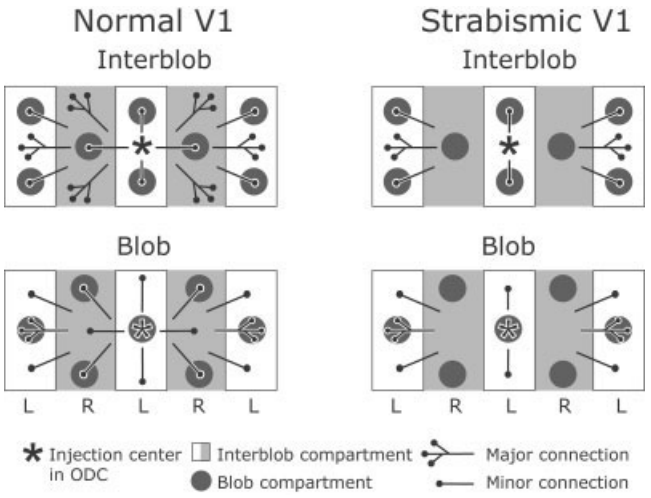

Fig. 10. Schematic view of horizontal patchy connections between ocular dominance columns (ODCs) in superficial layers of V1, normal vs. strabismic primate. In primate with normal binocular vision (left column), the majority of interblob neurons connect with other interblob neurons, and the majority of blob neurons connect with other blob neurons. The preference for "same cytochrome oxidase (CO) compartment" connection is strong-but-not-absolute, as illustrated by major vs. minor projections. Blob connections also show a monocular bias, i.e., the major projection is to blob compartments in ODCs with the same ocularity. In primates with infantile strabismus (right column), CO-compartmental specificity of connections is comparable to that in normal primate, but the monocular bias is more pronounced, especially for interblob compartment connections. R, right eye ODCs; L, left eye ODCs.

because the monkeys would retain connections between orientation-tuned interblob regions (Livingstone and Hubel, 1984a; Malach et al., 1993) belonging to the same eye. Lack of long-range, excitatory horizontal connections between the superficial layers of opposite-eye ODCs would be expected to impair binocular fusion and disparity sensitivity (Chino et al., 1996; Kumagami et al., 2000) and could explain behavioral deficits of stereoscopic perception and fusional vergence eye movements. A paucity of V1 binocular connections, convolved on innate, ipsiversive directional biases of pursuit-related neurons within each cerebral hemisphere, may also explain the directional deficits of smooth pursuit and fixation nystagmus that typify infantile strabismus (Tychsen and Lisberger, 1986; Kiorpes et al., 1996; Tychsen, 1999).

ACKNOWLEDGMENTS

We thank Drs. Greg DeAngelis and David Van Essen for many helpful comments, Dr. Ronald G. Boothe for important historical data on the strabismic animals, and Dr. Mae Gordon for help with statistical analysis. Xiao-Ping Jiang and Almi Rivera provided excellent technical assistance.

LITERATURE CITED

Adams DL, Horton JC. 2003. A precise retinotopic map of primate striate cortex generated from the representation of angioscotomas. J Neurosci 23:3771–3789.

Amir Y, Harel M, Malach R. 1993. Cortical hierarchy reflected in the organization of intrinsic connections in macaque monkey visual cortex. J Comp Neurol 334:19–46.

Angelucci A, Levitt JB, Walton EJ, Hupe JM, Bullier J, Lund JS. 2002. Circuits for local and global signal integration in primary visual cortex. J Neurosci 22:8633–8646.

Birch EE, Stager DR. 1985. Monocular acuity and stereopsis in infantile esotropia. Invest Ophthalmol Vis Sci 26:1624–1630.

Birch EE, Stager DR, Berry P, Everett ME. 1990. Prospective assessment of acuity and stereopsis in amblyopic infantile esotropes following early surgery. Invest Ophthalmol Vis Sci 31:758–765.

Birch EE, Fawcett S, Stager DR. 2000. Why does early surgical alignment improve stereopsis outcomes in infantile esotropia? J Am Assoc Pediatr Ophthalmol Strabismus 4:10–14.

Boothe RG, Quick MV, Joosse MV, Abbas MA, Anderson DC. 1990. Accessory lateral rectus orbital geometry in normal and naturally strabismic monkeys. Invest Ophthalmol Vis Sci 31:1168–1174.

Callaway EM. 1998. Local circuits in primary visual cortex of the macaque monkey. Annu Rev Neurosci 21:47–74.

Chavasse F. 1939. Worth's squint or the binocular reflexes and the treatment of strabismus. London: Bailliere Tindall and Cox.

Chino Y, Smith EL, Hatta S, Cheng H. 1996. Suppressive binocular interactions in the primary visual cortex (V1) of infant rhesus monkeys. Washington, DC: Society for Neuroscience. p 131.

Chino YM, Smith EL III, Hatta S, Cheng H. 1997. Postnatal development of binocular disparity sensitivity in neurons of the primate visual cortex. J Neurosci 17:296–307.

Crawford MLJ, Von Noorden GK. 1979. The effects of short-term experimental strabismus on the visual system in Macaca mulatta. Invest Ophthalmol Vis Sci 18:496–505.

Cumming BG, DeAngelis GC. 2001. The physiology of stereopsis. Annu Rev Neurosci 24:203–238.

Fenstemaker SB, Kiorpes L, Movshon JA. 2001. Effects of experimental strabismus on the architecture of macaque monkey striate cortex. J Comp Neurol 438:300–317.

Fisken RA, Garey LJ, Powell TPS. 1973. Patterns of degeneration after intrinsic lesions of the visual cortex (area 17) of the monkey. Brain Res 53:208–213.

Fisken RA, Garey LJ, Powell TPS. 1975. The intrinsic, association and commissural connections of area 17 of the visual cortex. Philos Trans R Soc B 272:487–536.

Hawken MJ, Parker AJ, Lund JS. 1988. Laminar organization and contrast sensitivity of direction-selective cells in the striate cortex of the old world monkey. J Neurosci 8:3541–3548.

Hebb DO. 1949. The organization of behavior—a neuropsychological theory. New York: John Wiley and Sons.

Horton JC, Hubel DH. 1981. Regular patchy distribution of cytochrome oxidase staining in primary visual cortex of macaque monkey. Nature 292:762–764.

Horton JC, Hocking DR, Adams DL. 1999. Metabolic mapping of suppression scotomas in striate cortex of macaques with experimental strabismus. J Neurosci 19:7111–7129.

Hoyt WF, Luis O. 1962. Visual fiber anatomy in the infrageniculate pathway of the primate. Arch Ophthalmol 68:124–136.

Hubel DH, Wiesel TN. 1965. Binocular interaction in striate cortex of kittens reared with artificial squint. J Neurophysiol 28:1041–1059.

Hubel DH, Wiesel TN. 1968. Receptive fields and functional architecture of monkey striate cortex. J Physiol 195:215–243.

Hubel DH, Wiesel TN. 1969. Anatomical demonstration of columns in the monkey striate cortex. Nature 221:747–750.

Hubel DH, Wiesel TN. 1977. Ferrier lecture. Functional architecture of macaque monkey visual cortex. Proc R Soc Lond B 198:1–59.

Jiang X, Johnson RR, Burkhalter A. 1993. Visualization of dendritic morphology of cortical projection neurons by retrograde axonal tracing. J Neurosci Methods 50:45–60.

Katz LC, Crowley JC. 2002. Development of cortical circuits: lessons from ocular dominance columns. Nature 3:34–42.

Kiorpes L, Boothe RG. 1981. Naturally occurring strabismus in monkeys (Macaca nemestrina). Invest Ophthalmol Vis Sci 20:257–263.

Kiorpes L, Walton PJ, O'Keefe LP, Movshon JA, Lisberger SG. 1996. Effects of artificial early-onset strabismus on pursuit eye movements and on neuronal responses in area MT of macaque monkeys. J Neurosci 16:6537–6553.

Kono R, Poukens V, Demer JL. 2002. Quantitative analysis of the structure of the human extraocular muscle pulley system. Invest Ophthalmol Vis Sci 43:2923–2932.

Kumagami T, Zhang B, Smith EL III, Chino YM. 2000. Effect of onset age of strabismus on the binocular responses of neurons in the monkey visual cortex. Invest Ophthalmol Vis Sci 41:948–954.

LeVay S, Stryker MP, Schatz CJ. 1978. Ocular dominance columns and their development in layer IV of the cat's visual cortex: a quantitative study. J Comp Neurol 179:223–244.

LeVay S, Connolly M, Houde J, Van Essen DC. 1985. The complete pattern of ocular dominance stripes in the striate cortex and visual field of the macaque monkey. J Neurosci 5:486–501.

Livingstone MS, Hubel DH. 1984a. Anatomy and physiology of a color system in the primate visual cortex. J Neurosci 4:309–356.

Livingstone MS, Hubel DH. 1984b. Specificity of intrinsic connections in primate primary visual cortex. J Neurosci 4:2830–2835.

Lowel S, Singer W. 1992. Selection of intrinsic horizontal connections in the visual cortex by correlated neuronal activity. Science 255:209–212.

Lund JS, Yoshioka T, Levitt JB. 1993. Comparison of intrinsic connectivity in different areas of macaque monkey cerebral cortex. Cereb Cortex 3:148–162.

Malach R, Amir Y, Harel M, Grinvald A. 1993. Relationship between intrinsic connections and functional architecture revealed by optical imaging and in vivo targeted biocytin injections in primate striate cortex. Proc Natl Acad Sci U S A 90:10469–10473.

Malpeli J, Baker F. 1975. The representation of the visual field in the lateral geniculate nucleus of Macaca mulatta. J Comp Neurol 161:569–594.

McLean IW, Nakane PPK. 1974. Periodate-lysine-paraformaldehyde fixative. A new fixation for immunoelectron microscopy. J Histochem Cytochem 22:1077–1083.

Norcia AM, Garcia H, Humphry R, Holmes A, Hamer RD, Orel-Bixler D. 1991. Anomalous motion VEPs in infants and in infantile esotropia. Invest Ophthalmol Vis Sci 32:436–439.

Rockland KS, Lund JS. 1983. Intrinsic laminar lattice connections in primate visual cortex. J Comp Neurol 216:303–318.

Roelfsema PR, Konig P, Engel AK, Sireteanu R, Singer W. 1994. Reduced synchronization in the visual cortex of cats with strabismic amblyopia. Eur J Neurosci 6:1645–1655.

Rubenstein R, Lohr K, Brook R, Goldberg G, Kamberg C. 1985. Measure-

ment of physiological health for children. Vol. 4. Vision impairments. Santa Monica: Rand Corporation.

Schor CM, Levi DM. 1980. Disturbances of small-field horizontal and vertical optokinetic nystagmus in amblyopia. Invest Ophthalmol Vis Sci 19:668–683.

Schor CM, Fusaro RE, Wilson N, McKee SP. 1997. Prediction of early-onset esotropia from components of the infantile squint syndrome. Invest Ophthalmol Vis Sci 38:719–740.

Sincich LC, Horton JC. 2002. Divided by cytochrome oxidase: a map of the projections from V1 to V2 in macaques. Science 295:1734–1737.

Tootell RBH, Hamilton SL, Silverman MS, Switkes E. 1988. Functional anatomy of macaque striate cortex. I. Ocular dominance, binocular interactions, and baseline conditions. J Neurosci 8:1500–1530.

Trachtenberg JT, Stryker MP. 2001. Rapid anatomical plasticity of horizontal connections in the developing visual cortex. J Neurosci 28:3476–3482.

Ts'o DY, Gilbert CD. 1988. The organization of chromatic and spatial interactions in the primate striate cortex. J Neurosci 8:1712–1727.

Ts'o DY, Gilbert CD, Wiesel TN. 1986. Relationships between horizontal interactions and functional architecture in cat striate cortex as revealed by cross-correlation analysis. J Neurosci 6:1160–1170.

Tychsen L. 1999. Infantile esotropia: current neurophysiologic concepts. In: Rosenbaum AL, Santiago AP, editors. Clinical strabismus management. Philadelphia: WB Saunders. p 117–138.

Tychsen L, Burkhalter A. 1995. Neuroanatomic abnormalities of primary visual cortex in macaque monkeys with infantile esotropia: preliminary results. J Pediatr Ophthalmol Strabismus 32:323–328.

Tychsen L, Burkhalter A. 1997. Nasotemporal asymmetries in V1: ocular dominance columns of infant, adult, and strabismic macaque monkeys. J Comp Neurol 388:32–46.

Tychsen L, Lisberger SG. 1986. Maldevelopment of visual motion processing in humans who had strabismus with onset in infancy. J Neurosci 6:2495–2508.

Tychsen L, Scott C. 2003. Maldevelopment of convergence eye movements in macaque monkeys with small- and large-angle infantile esotropia. Invest Ophthalmol Vis Sci 44:3358–3368.

Tychsen L, Hurtig RR, Scott WE. 1985. Pursuit is impaired but the vestibulo-ocular reflex is normal in infantile strabismus. Arch Ophthalmol 103:536–539.

Tychsen L, Rastelli A, Steinman S, Steinman B. 1996. Biases of motion perception revealed by reversing gratings in humans who had infantile-onset strabismus. Dev Med Child Neurol 38:408–422.

Tychsen L, Yildirim C, Anteby I, Boothe R, Burkhalter A. 2000. Macaque monkey as an ocular motor and neuroanatomic model of human infantile strabismus. In: Lennerstrand G, Ygge J, editors. Advances in strabismus research: basic and clinical aspects. London: Wenner-Gren International Series, Portland Press Ltd. p 103–119.

Van Essen DC. 1985. Functional organization of primate visual cortex. In: Peters A, Jones E, editors. Cerebral cortex. New York: Plenum Press. p 259–329.

Van Essen DC, Newsome WT, Maunsell JHR. 1984. The visual field representation in striate cortex of the macaque monkey: asymmetries, anisotropies, and individual variability. Vision Res 24:429–448.

Van Sluyters RC, Levitt FB. 1980. Experimental strabismus in the kitten. J Neurophysiol 43:686–699.

von Noorden GK. 1996. Binocular vision and ocular motility. St. Louis: Mosby Year Book, Inc.

Wiesel TN. 1982. Postnatal development of the visual cortex and the influence of environment. Nature 299:583–591.

Wong AMF, Lueder GT, Burkhalter A, Tychsen L. 1998. Anomalous retinal correspondence: neuroanatomic mechanism in strabismic monkeys and clinical findings in strabismic children. J Am Assoc Pediatr Ophthalmol Strabismus 4:168–174.

Wong AMF, Foeller P, Bradley D, Burkhalter A, Tychsen L. 2003. Early versus delayed repair of infantile strabismus in macaque monkeys: I. Ocular motor effects. J Am Assoc Pediatr Ophthalmol Strabismus 7:200–209.

Worth C. 1903. Squint. Its causes, pathology, and treatment. Philadelphia: Blakiston.

Wright KW, Edelman PM, McVey JH, Terry AP, Lin M. 1994. High-grade stereo acuity after early surgery for congenital esotropia. Arch Ophthalmol 112:913–919.

Yoshioka T, Blasdel GG, Levitt JB, Lund JS. 1996. Relation between patterns of intrinsic lateral connectivity, ocular dominance, and cytochrome oxidase-reactive regions in macaque monkey striate cortex. Cereb Cortex 6:297–310.